Proceedings Paper:

Ponce, R, Sharif-Azadeh, S, Stange, D et al. (5 more authors) (2017) Design of a high-speed germanium-tin absorption modulator at mid-infrared wavelengths. In: IEEE 14th International Conference on Group IV Photonics (GFP 2017). GFP 2017, 23-25 Aug 2017, Berlin, Germany. , pp. 19-20. ISBN 978-1-5090-6568-4

https://doi.org/10.1109/GROUP4.2017.8082175

Design of a high-speed germanium-tin absorption modulator at mid-infrared wavelengths

R. Ponce[1,2,3], S. Sharif Azadeh[1,3], D. Stange[2,3], F. Merget[1,3], B. Marzban[1,3], Z. Ikonic[4], D. Buca[2,3], J. Witzens[1,3]

[1]Institute of Integrated Photonics, RWTH Aachen University, Sommerfeldstraße 18/24, 52074 Aachen, Germany
[2]Peter Grünberg Institute 9 (PGI 9), Forschungszentrum Jülich, 52425 Jülich, Germany
[3]Jülich Aachen Research Alliance, Fundamentals of Future Information Technology (JARA-FIT)
[4]Institute of Microwaves and Photonics, University of Leeds, Leeds LS29JT, UK

We propose a high-speed electro-absorption modulator based on a direct bandgap $Ge_{0.875}Sn_{0.125}$ alloy operating at mid-infrared wavelengths. Enhancement of the Franz-Keldysh-effect by confinement of the applied electric field to GeSn in a reverse-biased junction results in 3.2dB insertion losses, a 35GHz bandwidth and a 6dB extinction ratio for a $2V_{pp}$ drive signal.

Extension of Silicon Photonics to the longer wavelength IRB and mid-IR regions has attracted very considerable attention in recent years [1]. The recent demonstration of a direct bandgap Germanium-Tin (GeSn) IRB laser [2],[3] offers the prospect of establishing a complete group IV mid-IR platform, provided reliable electrically pumped room temperature lasing can be reached. Important progress has already been made on extended wavelength GeSn photodetectors [4],[5]. On the other hand, only a few studies have been made on the realization of GeSn modulators. Theoretical studies have been mostly focusing on the physical modelling of direct absorption via the quantum confined Stark effect [6],[7] or the Franz-Keldysh effect (FKE) [8], rather than a comprehensive device design relying on a proven fabrication flow. We propose a high-speed and low power consumption FKE GeSn modulator design relying on a strain relaxed $Ge_{0.875}Sn_{0.125}$ layer grown on a Ge virtual substrate (with a residual compressive strain of -0.4%), as already experimentally realized [3], with a room temperature direct bandgap of 440meV (absorption edge at 2.82μm). The modulator is based on a vertical 1μm/300nm/300nm Ge/GeSn/SiGeSn stack grown on Si, in which the upper SiGeSn and the lower Ge layers are respectively intentionally n-doped to 1e18cm^{-3} (top 30nm n-doped to 2e19cm^{-3} to facilitate top contacting) and p-doped to 3e16cm^{-3}. The GeSn is intrinsically p-type (~1e17cm^{-3}) due to native point defects. Application of a reverse bias across the stack partially depletes the GeSn layer and results in the application of an electric field in the space charge region, so that both the FKE and free carrier absorption contribute to the variable absorption. Under application of a reverse biased voltage, the induced change of free carrier absorption is opposite to that of FKE. It has, however, also a much smaller magnitude at the chosen bias point. n-doping of the topmost SiGeSn is chosen at least an order of magnitude above the native GeSn n-doping to ensure that the applied field is primarily localized in the latter. Assumed refractive indices are 4.02 (Ge), 4.2 (GeSn) and 4.02 (SiGeSn).

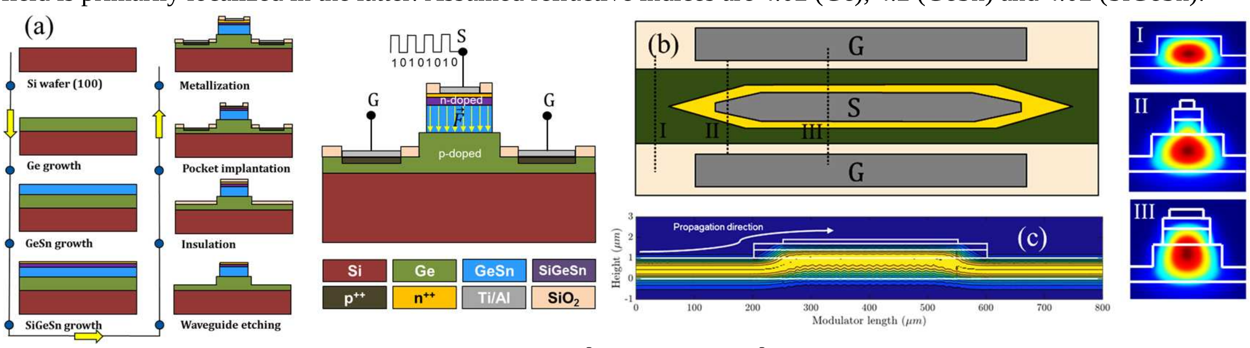

Fig. 1. (a) GeSn modulator fabrication flow ($p_{Ge\text{-}VS}$: 3e16cm^{-3}, n_{SiGeSn}: 1e18cm^{-3}). (b) Top view of the modulator. The optical mode is shown at 3 different cross-sections of the device: I) Ge interconnect waveguide, II) inside the taper and III) main section of the modulator. (c) Vertical cross-section of the modulator showing the optical field along the device, from beam-prop simulations.

Fig. 1 is a schematic representation of the device. The GeSn/SiGeSn layers are removed everywhere except in the active region of the device to enable reduced loss, 2 μm wide Ge single mode interconnect waveguides (p-doping still results in ~2.3dB/mm) defined by a 600nm deep etch into the Ge (400nm slab thickness). The GeSn/SiGeSn stack is tapered up to a 1.4μm width in a 50μm long transition that allows adiabatically pulling up the field into the GeSn region. A central electrode on top of the stack allows contacting the cathode. Further device designs relying on segmented waveguides [9] for contacting without metal induced excess losses, as well as on a p-SiGeSn/GeSn/n-SiGeSn stack grown on intrinsic Ge for low loss interconnect waveguides are currently under study. The optimization of phase shifters with the same waveguide configuration is also under study and will be reported at the conference.

The FKE is modelled based on Eq. 6 in [8], with the value of the parameter C used therein taken from the same reference. Due to the residual compressive strain, the light hole and heavy hole bands are split. Only the heavy hole band, preferentially interacting with TE polarized light, is taken into account. The effective masses were calculated using the 8 band k·p method, resulting in $0.22m_0$ for the heavy hole effective mass and $0.03m_0$ for the Γ-valley electron mass, both taken in the growth direction along which the electric field is applied. Fig. 2(a) shows the calculated change in absorption ($\Delta\alpha$) induced in the GeSn alloy by the applied electric field as a function of photon energy, and Fig. 2(b) shows the induced refractive index change calculated with the same model [8],[10]. Sub-bandgap absorption (Urbach tail) was taken from [11] (data for 11% shifted by the change in bandgap). Free carrier absorption and electro-refraction are estimated based on a corrected, empirical Drude model [12]. In line with what is seen for electron mediated losses in Ge and hole mediated losses in Si, theoretically predicted absorption losses are doubled. In addition, inter-valence band absorption seen in Ge (~400dB/cm at 1e18cm^{-3} hole concentration) [13] is also assumed here in the GeSn film and intra-conduction band absorption seen in Si (~90dB/cm at 1e18cm^{-3}) is also assumed here in the SiGeSn film. Correction factors to the Drude model for free carrier induced electro-refraction are respectively assumed to be 0.6 for electrons and 0.9 for holes, in line with the Ge coefficients.

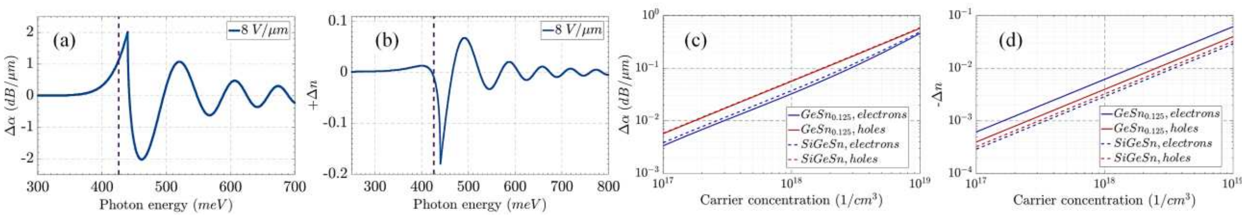

Fig. 2. Prediction of FKE in $Ge_{0.875}Sn_{0.125}$ under 8 $V/\mu m$: (a) electro-absorption and (b) electro-refraction. (c) and (d) show the absorption and refractive index change due to free carriers at the photon energy E_g – 10meV.

Although the intrinsic figure of merit $\Delta\alpha/\alpha$ peaks at a larger optical carrier detuning below the bandgap energy [14], once excess optical losses due to doping and metal contacting are taken into account, the optimal optical carrier photon energy was found to be about 10meV below the bandgap (E_g). Unlike $\Delta\alpha$, which is always positive below the bandgap, the FKE induced Δn changes sign at E_g – 10meV for an applied electrical field of 8V/μm (resulting from applying 2V reverse bias to the device), meaning that low chirp operation can also be achieved since the dominant electro-refraction effect is also zeroed close to that energy. Short devices with high $\Delta\alpha$ resulting from optical carrier frequencies close to the bandgap energy are required due to the high excess losses. This has also the side benefit of high bandwidth, especially since we assume the modulator to be driven as a lumped element with a 50Ω driver and thus the bandwidth is mainly determined by the capacitance of the device.

The performance metrics of the modulator are calculated by simulating the diode at different applied voltage levels, calculating the carrier and field distributions and the resulting change of the complex refractive index, and subsequently the effective index change based on the optical overlap with the different regions. Table 1 summarizes the calculated characteristics of the modulator.

Wavelength	*Length (incl. taper)*	*V_{pp} and DC V_{bias}*	*Extinction Ratio*	*Insertion Loss*	*Power consumption*	*Bandwidth*
2.88 μm	102 μm	$2V_{pp}$ @-1V	6.0 dB	3.2 dB	70 fJ/bit	35 GHz

Table 1. Summary of the modeled modulator characteristics.

References

[1] G. Mashanovich et al., “Germanium Mid-Infrared Photonic Devices,” J. Lightwave Technol., vol. 35, pp. 624-630, 2017.
[2] S. Wirths et al., “Lasing in direct-bandgap GeSn alloy grown on Si,” Nat. Photon., vol. 9, pp. 88-99, 2015.
[3] D. Stange et al., “Optically pumped GeSn Microdisk Lasers on Si,” ACS Photon., vol. 3, pp. 1279-1285, 2016.
[4] T. Pham et al., “Systematic study of Si-based GeSn photodiodes with 2.6 μm detector cutoff for short-wave infrared detection,” Opt. Express, vol. 24, pp 4519-4531, 2016.
[5] M. Oehme et al., “GeSn/Ge multiquantum well photodetectors on Si substrates,” Opt. Lett., vol. 39, pp. 4711-4714, 2014.
[6] T. Fujisawa, K. Saitoh, “Quantum-Confined Stark Effekt Analysis of GeSn/SiGeSn Quantum Wells for Mid-Infrared Si-Based Electroabsorption Devices Based on Many-Body Theory,” J. Quant. Electron., vol. 51, no. 11, Nov. 2015, Art. ID 8400207.
[7] N. Yahyaoui et al., “Stark shift of the absorption spectra in Ge/$Ge_{1-x}Sn_x$/Ge type-I single QW cell for mid-wavelength infra-red modulators,” Superlattices Microst., vol 85, pp. 629-637, 2015.
[8] R. A. Soref et al., “Franz-Keldysh electro-absorption modulation in germanium-tin alloys,” J. Appl. Phys., vol 111, Art. ID 123113, 2012.
[9] M. Hochberg et al., “Segmented waveguides in thin silicon-on-insulator,” J. Opt. Soc. Am. B, vol. 22, pp. 1493-1497, 2005.
[10] B. R. Bennett et al., “Electrorefraction and Electroabsorption in InP, GaAs, GaSb, InAs, and InSb,” J. Quant. Electron., vol. 23, pp. 2159-2166, 1987.
[11] G. He et al., “Interband Transitions in Sn_xGe_{1-x} Alloys,” Phys. Rev. Lett., vol. 79, pp. 1937-1940, 1997.
[12] M. Nedeljkovic, R. Soref, and G. Z. Mashanovich, “Free-carrier electrorefraction and electroabsorption modulation predictions for silicon over the 1.3–14 um infrared wavelength range,” IEEE Photon. J., vol. 3, no. 6, pp. 1171–1180, Dec. 2011.
[13] M. Nedeljkovic et al., “Predictions of Free-Carrier Electroabsorption and Electrorefraction in Germanium,” Phot. J., vol. 7, no. 3, Jun. 2015, Art. ID 2600214.
[14] R. Soref, “Silicon-based silicon-germanium-tin heterostructure photonics,” Phil. Trans. R. Soc. A, vol. 372, Mar. 2014, Art. ID 20130113.